AMERICAN SOCIETY of
GENE & CELL
THERAPY

A Nanostructured Lipid Carrier for Delivery of a Replicating Viral RNA Provides Single, Low-Dose Protection against Zika

Jesse H. Erasmus,[1,4] Amit P. Khandhar,[1,4] Jeff Guderian,[1] Brian Granger,[1] Jacob Archer,[1] Michelle Archer,[1] Emily Gage,[1,2] Jasmine Fuerte-Stone,[1] Elise Larson,[1] Susan Lin,[1] Ryan Kramer,[1] Rhea N. Coler,[1,2,3] Christopher B. Fox,[1] Dan T. Stinchcomb,[1,5] Steven G. Reed,[1,2] and Neal Van Hoeven[1,2,3]

[1]Infectious Disease Research Institute, Seattle, WA, USA; [2]University of Washington, Department of Global Health, Seattle, WA, USA; [3]PAI Life Sciences Inc., Seattle, WA, USA

Since the first demonstration of *in vivo* gene expression from an injected RNA molecule almost two decades ago,[1] the field of RNA-based therapeutics is now taking significant strides, with many cancer and infectious disease targets entering clinical trials.[2] Critical to this success has been advances in the knowledge and application of delivery formulations. Currently, various lipid nanoparticle (LNP) platforms are at the forefront,[3] but the encapsulation approach underpinning LNP formulations offsets the synthetic and rapid-response nature of RNA vaccines.[4] Second, limited stability of LNP formulated RNA precludes stockpiling for pandemic readiness.[5] Here, we show the development of a two-vialed approach wherein the delivery formulation, a highly stable nanostructured lipid carrier (NLC), can be manufactured and stockpiled separate from the target RNA, which is admixed prior to administration. Furthermore, specific physicochemical modifications to the NLC modulate immune responses, either enhancing or diminishing neutralizing antibody responses. We have combined this approach with a replicating viral RNA (rvRNA) encoding Zika virus (ZIKV) antigens and demonstrated a single dose as low as 10 ng can completely protect mice against a lethal ZIKV challenge, representing what might be the most potent approach to date of any Zika vaccine.

INTRODUCTION

The periodic yet unpredictable nature of epidemic disease emergence presents a moving target that is not amenable to rapid prophylactic interventions given current vaccine development paradigms. A major hurdle to rapid clinical development of a vaccine candidate occurs during the process development stage. Modern protein-based vaccine platform technologies, such as subunit or viral-display strategies, that are modular in nature, allow for the standardization of upstream and downstream processes.[6,7] However, manufacturing relies heavily on cell- or tissue-based production schemes, and downstream purification tends to be antigen-dependent, requiring time-consuming optimization and validation. Nucleic acid-based vaccine platforms represent a sequence-independent platform with a universal produc-

tion process, significantly reducing time and cost to adapt the platform to a new target pathogen and offering an attractive approach for emerging infectious diseases. DNA and RNA have been extensively developed as vaccine platform technologies, with the former requiring nuclear delivery—a process that works efficiently in small-animal models but is highly inefficient in larger-animal models, including humans, often requiring very high doses and posing some safety concerns.[8,9] Conversely, RNA only requires cytoplasmic delivery and has proven effective in both small- and large-animal models.[4,10–12] RNA-based technologies include non-replicating platforms that are optimized for expression and/or modified to avoid immune detection or replicating platforms that utilize viral replication machinery to balance the stimulation of innate immunity against viral protein-dependent innate immune antagonism, resulting in a self-adjuvating and robust antigen expression profile.

RNA-based therapeutics have had a slow coming of age because of the molecule's notorious instability *in vivo*. Given its unstable nature, coupled with the requirement for transport across a lipid bilayer for efficient antigen expression, delivery methods remain a major roadblock to the clinical evaluation of RNA platform technologies. Currently, protein or peptide-dependent (including viral delivery)[13–16] or lipid-based approaches are being investigated,[17–20] with the latter being more amenable to a rapid production platform for pandemic responses due to a cell-free production process. Lipid-based delivery approaches include lipid nanoparticles (LNPs) that are proving to be extremely effective but require the co-manufacture

of the delivery vehicle with the encapsulated target RNA, which can be difficult to scale and produce in a timely response to a pandemic.[17,20] Brito et al.[19] recently described an alternative emulsion-based delivery vehicle that utilizes the framework of the adjuvant MF59 and modifies it with the addition of the cationic lipid DOTAP (1,2-dioleoyl-3-trimethylammonium-propane, chloride salt). The resulting cationic nanoemulsion (CNE) binds RNA to the nanoparticle surface, allowing for the admixing of delivery vehicle and RNA at point of use. This two-vial approach would allow for the delivery vehicle to be stockpiled and mixed with any target RNA prior to administration, ideal for a pandemic response situation.

Considering recent zoonotic disease epidemics, including chikungunya, Ebola, and Zika, which may require potentially hundreds of millions of doses each, the need for such rapid-response platforms are becoming increasingly apparent. Zika has underscored the extent of the unpredictable nature of emerging viral diseases. Despite the first identification of Zika virus (ZIKV) in 1947, little progress was made in characterizing the viral pathogenesis, most likely due to the seemingly mild and self-limiting disease that ZIKV infection caused. However, since 2010, alarming observations have been made, including sexual transmission,[21] autoimmune syndromes,[22,23] and neurodevelopmental congenital malformations[24,25] following ZIKV infection. Convincing evidence has been accumulated that directly links these pathologies with ZIKV infection. In light of these recent findings, rapid progress in the development of vaccine candidates based on various platforms for Zika have been made by multiple research groups, including subunit,[26,27] inactivated,[28,29] live-attenuated,[30,31] and non-replicating nucleic acid approaches, which include DNA[29,32–34] and modified or optimized mRNA encapsulated in LNPs.[35–37] In order to provide an alternative approach to LNP encapsulated mRNA, we have engineered a platform that combines replicating viral RNA (rvRNA), derived from the alphavirus genus, with a nanostructured lipid carrier (NLC) delivery formulation, and applied the platform in the development of a Zika vaccine candidate.

NLCs represent a hybrid formulation between oil-in-water (o/w) emulsions and solid lipid nanoparticles (SLNs) and were historically developed for the delivery of lipophilic small-molecule drugs.[38] The nanoparticle core consists of a liquid oil phase, such as squalene, with a solid phase lipid composed of a saturated triglyceride. The hybrid nature of the core forms a semi-crystalline matrix that provides superior colloidal stability relative to o/w emulsions and, depending on the fraction of the solid lipid component, ease of manufacturability relative to SLNs. Here, we demonstrate physicochemical and biological optimization of NLC and rvRNA complexes to overcome practical and nontrivial challenges impeding clinical translation of RNA-based vaccines, to develop a formulation platform with four key characteristics: (1) is manufacturable and has stable formulation that can be stockpiled with flexibility to be admixed with the target rvRNA at the time of administration, (2) can be chemically modified to modulate immune response to rvRNA-encoded antigens, (3) has sufficient RNA-loading capacity to allow for flexibility in dose-finding studies, and 4) utilizes tolerable amounts of cationic lipid to deliver

effective doses of RNA. Using the platform, we have developed an efficacious rvRNA vaccine for ZIKV that requires reduced doses compared to other nucleic acid vaccine platforms.

RESULTS

Development of an rvRNA Construct Encoding ZIKV Pre-membrane and Envelope Genes

To produce self-replicating RNA encoding ZIKV antigens, we utilized the attenuated strain of Venezuelan equine encephalitis virus, TC-83, due to its safety record in clinical trials[39] (Figure 1A). We encoded pre-membrane (prM) and envelope (E) genes of French Polynesian ZIKV strain H/PF/2013[40] with an upstream homotypic ZIKV or heterotypic Japanese encephalitis virus (JEV) signal sequence into pT7-VEE-REP. A control reporter rvRNA, encoding secreted human embryonic alkaline phosphatase (SEAP) was also designed (Figure 1B). To confirm that our rvRNAs encoding ZIKV prM and E were functional and induced the secretion of virus-like particles (VLPs), we transfected 293T cells and analyzed supernatants following sucrose gradient sedimentation for the presence of VLPs by western blot (Figure 1C) and electron microscopy (Figure 1D).

Others have demonstrated that the JEV signal sequence enhances secretion of VLPs in the context of prM and E from dengue and West Nile virus, flaviviruses closely related to ZIKV.[41] To down select a single ZIKV rvRNA construct for continued development, we compared neutralizing antibody (nAb) responses between rvRNAs encoding ZIKV prM and E with native as well as JEV signal sequences. The native ZIKV signal sequence construct induced 100% seroconversion after a single dose and significantly higher nAb titers after two doses compared to the rvRNA encoding the JEV signal sequence (Figure S1).

Development of NLCs with Varying Physicochemical Properties

NLCs consist of a blend of solid lipid (glyceryl trimyristate-dynasan 114) and liquid oil (squalene) (Figure 2A), which forms a semi-crystalline core upon emulsification. Figure 2B compares the particle size distribution, measured using dynamic light scattering (DLS), between an NLC and CNE formulation at the time of manufacturing. Since long-term colloidal stability was a prerequisite for us to develop formulations that were suitable for stockpiling in a rapid-response scenario, we monitored average particle diameter of formulations stored at 25°C. Particle diameter of NLCs was nearly unchanged (<3% change) for at least 9 months compared to CNE, which increased 30% after 3 months and 350% after 9 months of storage (Figure 2C). The nonionic surfactants, which include the hydrophobic sorbitan ester (Span), the hydrophilic ethoxylated sorbitan ester (Tween), and the cationic lipid DOTAP, are critical to preserving colloidal stability, and due to their interfacial presence, play a key role in governing biophysical interactions. As a result, we sought to empirically elucidate the role of surfactants in mediating rvRNA protection, protein expression, and immunogenicity. NLCs of varying physicochemical properties were synthesized using a high-pressure microfluidization process (see Materials and Methods). Compositions of exemplary NLC formulations and a CNE formulation,
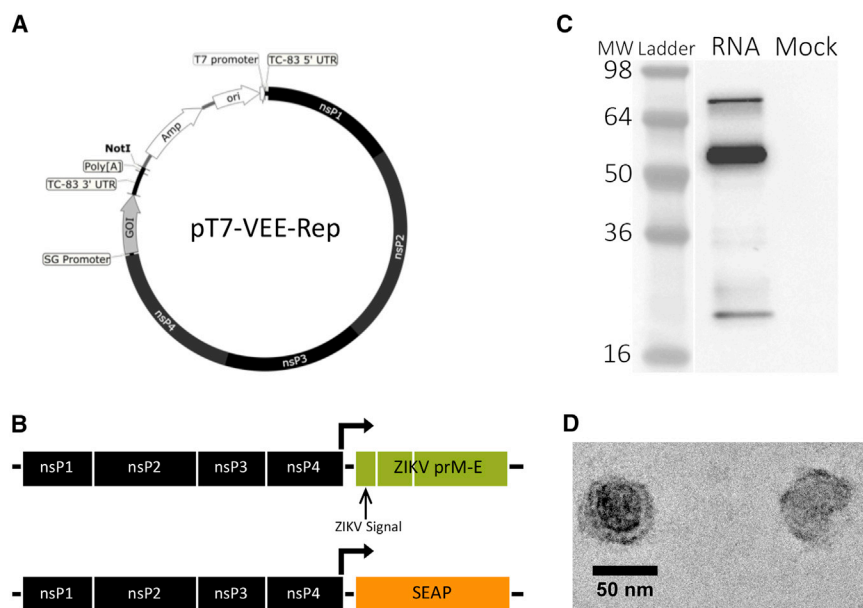
A

B

C

D

Figure 1. Design and Qualification of ZIKV rvRNA

(A) Plasmid DNA encoding a Venezuelan equine encephalitis replicon derived from the vaccine strain TC-83 under the control of a T7 RNA polymerase promoter. Subgenomic, SG; gene of interest, GOI. (B) Design of replicating viral RNAs encoding pre-membrane (prM) and envelope (E) genes of ZIKV strain H/PF/2013 or secreted human embryonic alkaline phosphatase (SEAP). Supernatants of 293T cells transfected with ZIKV or SEAP rvRNA were analyzed for the presence of Zika virus-like particles following sedimentation through 30% sucrose by ultracentrifugation. (C) Western blot of pelleted samples under denaturing conditions using polyclonal antibodies against ZIKV demonstrated reactivity against proteins corresponding to prM (21 kDa), E (54 kDa), or unprocessed prM-E fusion (76 kDa). (D) Transmission electron microscopy of pelleted samples following negative staining.

manufactured in-house according to a previously published method,[19] are summarized in Table 1. Increasing the surfactant-to-oil (S:O) molar ratio reduced particle size (Figure S2), which allowed us to generate unimodal NLCs with Z-average diameter ranging from 40 to 100 nm, as measured by DLS. Zeta potential correlated with the amount of DOTAP, increasing from approximately +15 mV with 0.4% w/v DOTAP to +28 mV with 3.0% w/v DOTAP.

Physical Characterization of NLC-rvRNA Complexes *In Vitro*

We incubated rvRNA with NLCs of varying compositions in the presence or absence of RNase A and evaluated integrity of the extracted RNA using denaturing agarose gel electrophoresis. We established that certain compositional requirements were essential for RNA protection; specifically, NLCs with a relatively high Tween 80 content (70% of total surfactant and cationic lipid mass) did not protect against RNase degradation (Figure S3A) and could not deliver rvRNA *in vivo* (Figure S3B). Conversely, NLCs with relatively lower Tween 80 fraction in the surfactant phase (35% of total surfactant and cationic lipid mass) protected rvRNA from degradation (Figure 2D). As a result, subsequent studies were conducted with NLCs containing Tween 80 no greater than 35% of the total surfactant fraction, subsequently referred to as NLC_{v1}. Next, we sought to optimize the complexing conditions, as measured by the nitrogen (N) to phosphate (P) molar ratio (N:P), to maximize transfection *in vitro*. CNE or NLC_{v1} formulations were complexed with rvRNA encoding SEAP at a range of N:P values and 100 ng of each rvRNA complex was incubated with baby hamster kidney (BHK) cells overnight. We compared SEAP expression as a function of N:P between NLC_{v1} and CNE (Figure 2E). As N:P increased, we observed escalating levels of SEAP with significantly higher expression with CNE compared to NLC_{v1} at N:P < 50. However, at N:P ~50, SEAP expression with CNE peaked, decreasing at N:P > 50, potentially due to cytotoxicity evidenced by

significant cellular detachment. Interestingly, at N:P ~50, SEAP expression in the NLC_{v1} group was similar to CNE and continued to increase. For downstream comparison studies between NLC_{v1} and CNE, we utilized an N:P of 50, which resulted in similar SEAP expression levels *in vitro*.

Formulation Composition Effects on Immune Responses to NLC-rvRNA Complexes

To evaluate the role of the nonionic Span surfactant, we synthesized two variants of NLC_{v1}, replacing Span 60 with either Span 80 or Span 85; we did not observe any detrimental effects on colloidal stability as a result. C57BL/6 mice were injected intramuscularly (IM) with 100 ng SEAP-rvRNA formulated with each NLC and compared with rvRNA formulated with CNE or unformulated rvRNA (Figure 3A). SEAP activity in serum harvested 3 days after injection was enhanced over 25-fold in all formulated rvRNA groups, including NLCs and CNE, compared to unformulated rvRNA, but expression levels were not different between rvRNA-formulated NLCs containing various Span surfactants or CNE-formulated rvRNA (Figure 3A).

In complementary experiments, we immunized C57BL/6 mice via the IM route with 100 ng of ZIKV-rvRNA, formulated with either NLC_{v1}, its Span 80 or Span 85 variants, CNE, or unformulated (naked) and compared nAb titers 14 days after a single dose. In contrast to the *in vivo* SEAP expression experiment, we observed significant differences in nAb responses (Figure 3B). NLC_{v1} with Span 60 elicited significantly higher nAb titers compared to CNE, NLC with Span 85, or NLC with Span 80. Since SEAP expression levels between the different formulation groups were identical (Figure 3A), differences in nAb titers were likely due to differences in the hydrophobic surfactant identity. To confirm that protein expression levels between CNE and NLC_{v1} were not changing over time, we immunized C57BL/6 with 100 ng of formulated or unformulated SEAP rvRNA and measured SEAP activity in serum harvested at days 3, 7, 14, 21, and
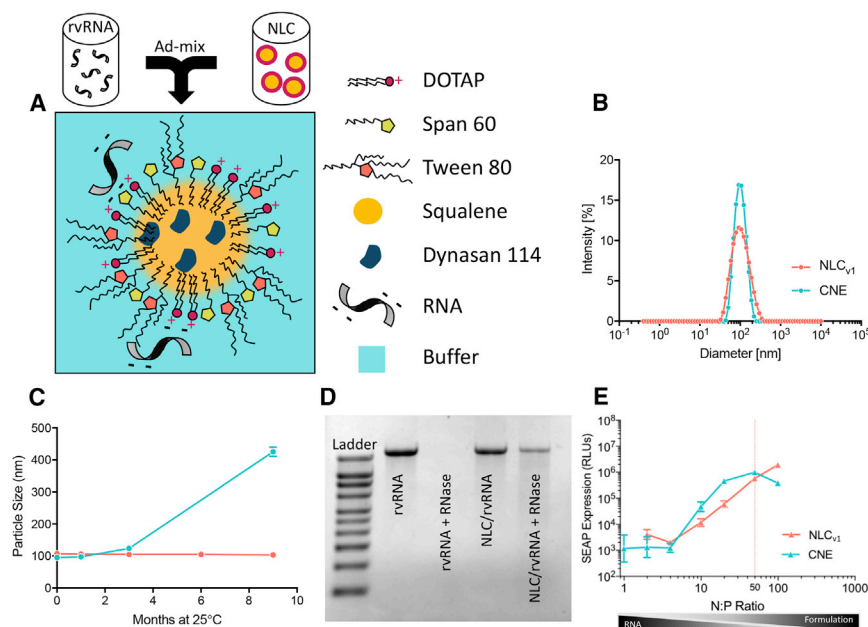
Figure 2. Overview of the NLC Formulation for RNA Delivery

(A) Schematic representation of rvRNA surface adsorbed to NLC nanoparticle post-admixture. The following physical and biophysical properties of NLC$_{v1}$ and CNE were compared: (B) intensity weighted size distribution, (C) particle size (Z-average diameter) evolution over 9 months to evaluate colloidal stability of formulations stored at 25°C, (D) protection from RNase, and (E) in vitro SEAP expression (relative luminescence units, RLUs) as a function of the molar ratio of formulation nitrogen (N) to RNA phosphate (P) values.

was replaced with a medium-chain-length triglyceride oil (Miglyol 810) to see if a squalene-based emulsion was necessary for the adjuvant effect. Twenty-four hours later, we harvested supernatants and measured the quantity of Mip-1β by ELISA (Figure 3D). Only squalene-based emulsions containing Dynasan 114 and the hydrophobic surfactant Span 60 or Span 85 enhanced the secretion of Mip-1β compared to CNE or naked rvRNA groups, with mean concentrations of 1,813 and 1,664 pg/mL compared to 179 and 110 pg/mL, respectively.

28 after injection (Figure S4)—no significant differences were observed between CNE and NLC$_{v1}$ groups.

To investigate whether replacing Span 85 in CNE with Span 60 also enhances immunogenicity, we immunized mice via the IM route with 100 ng ZIKV-rvRNA formulated with CNE containing either Span 85 or Span 60. Note that replacing Span 85 with Span 60 did not significantly affect average particle size but did improve long-term colloidal stability—CNE containing Span 60 grew 10% in average particle size after 3 months at 25°C compared to 30% when containing Span 85. For comparison and repetition, we included groups immunized with ZIKV-rvRNA formulated with either NLC$_{v1}$ or its Span 85 variant. Serum nAb activity was then assayed 14 days later. While rvRNA formulated with NLC or CNE containing Span 85 induced similar nAb activity (Figure 3C), Span 60 produced a differential effect, significantly enhancing nAb activity in the NLC$_{v1}$ group while diminishing nAb activity in the CNE group.

Since we observed differential immunogenicity despite similar protein expression levels, we hypothesized that certain formulation compositions were enhancing or adjuvanting the immune response. Given the similarities with MF59 (5% v/v squalene, 0.5% w/v Tween 80, 0.5% w/v Span 85), a well-characterized o/w emulsion adjuvant that enhances antigen-specific immune responses by inducing chemokine secretion, including macrophage inflammatory protein (Mip)-1β,[42–44] we hypothesized that certain compositions—particularly, based on the results above, compositions containing Dynasan 114 and Span 60—would also enhance chemokine secretion. To test this hypothesis, we complexed rvRNA with CNEs or NLCs manufactured with various hydrophobic surfactants and incubated with human peripheral blood mononuclear cells (PBMCs) from six donors. We also included an NLC where the squalene oil component

NLC-Formulated rvRNA Provides Dose-Dependent Long-Term Immunogenicity and Efficacy

Whereas C57BL/6 mice are immunocompetent and thus ideal for evaluating immunogenicity, assessing efficacy is complicated due to their relative resistance to ZIKV infection.[45] We utilized a previously described method[46] that includes the administration of an interferon alpha receptor (IFNAR) blocking monoclonal antibody 1 day before as well as 1 and 4 days after challenge in order to increase the susceptibility of C57BL/6 mice to ZIKV Dakar strain 41525. Based on the above data, we utilized Span 60 as the hydrophobic surfactant in NLC$_{v1}$ and evaluated the effect of 1- or 0.1-μg doses of rvRNA on nAb kinetics following prime only or prime-boost vaccination. C57BL/6 were immunized with 1 or 0.1 μg of rvRNA formulated with NLC$_{v1}$ and compared to unformulated 10-fold higher doses in two separate experiments, where one experiment assessed post-prime nAb titers, while the other included a boost vaccination at day 28. Mice were periodically bled, and nAb titers were assessed by 80% plaque-reduction neutralization tests (PRNT$_{80}$) (Figure 4). In both experiments, we observed peak nAb titers at day 14, with the 0.1-μg formulated doses inducing significantly higher titers than the 1-μg formulated doses. However, by days 88, 156, and 225 after a single administration, the 0.1-μg formulated group exhibited a significant drop in nAb titers, compared to peak titers at day 14, in a similar manner to the 10-μg unformulated groups, while the 1-μg formulated group showed no significant change in titer until 225 days after a single immunization (Figure 4A). After boost immunization, we observed significant nAb titer decay between days 14, 126, 209, and 280, even with a booster immunization at day 28 in the 0.1-μg formulated

Table 1. Exemplary Formulation Compositions

Formulation	DOTAP (%w/v)	Span XX (%w/v)	Tween 80 (%w/v)	Squalene (%w/v)	Dynasan 114 (%w/v)	S:O ratio[a]	Z-average (nm) (PDI)	Zeta Potential (mV)
NLC_{v1}	0.4	Span 60: 0.5	0.5	4.75	0.25	0.18	91.90 (0.17)	15.60 ± 0.12
NLC_{v2}	3.0	Span 60: 3.7	3.7	3.75	0.25	1.68	40.55 (0.20)	28.4 ± 1.27
CNE	0.4	Span 85: 0.5	0.5	4.3	0.00	0.14	97.23 (0.06)	13.1 ± 3.25

$$^a - S:O\ (molar\ ratio) = \frac{[DOTAP] + [Span] + [Tween]}{[Squalene + Dynasan\ 114]}$$

group, while the 1-μg formulated group showed no significant change in titer after 280 days (Figure 4B).

To assess long-term efficacy, mice were challenged 32 weeks after a single immunization or 36 weeks after two immunizations and bled 4 days later to quantify viremia by plaque assay (Figures 4C and 4D). Body weights and survival were monitored daily; however, no weight loss or morbidity was observed in any groups, most likely due to the age and weight of these mice at the time of challenge (40–48 weeks), in contrast to challenge in younger mice as observed in the studies below. Despite their resistance to these symptoms of disease, we did observe high levels of viremia in mock or unformulated rvRNA immunized groups, while the 1- and 0.1-μg doses of NLC_{v1} formulated rvRNA significantly reduced viremia, with the higher dose protecting 100% of mice from detectable viremia (limit of detection = 50 plaque-forming units [PFU]/mL).

Optimization of RNA Loading Capacity

In anticipation of larger animal models and clinical studies that could require larger RNA doses, we next made modifications to our lead NLC_{v1} formulation that would increase the RNA loading capacity. In the above experiments, NLC_{v1} or CNE was mixed 1:1 with 40 μg/mL RNA (N:P = 50), which was the lowest concentration that (1) allowed for a 1-μg RNA dose in a 50-μL injection volume and (2) resulted in optimal SEAP expression in vitro (Figure 2E) and in vivo (Figure S5). However, an N:P value of 50 translates to a relatively large excess of formulation, which poses formulation-associated tolerability risks with increasing dose requirements; emulsified squalene and DOTAP (cationic lipids in general) are immunostimulants, and high amounts can induce inflammatory and local reactogenicity.[47,48] As a result, we sought to design and synthesize an NLC formulation that can deliver a high RNA dose at significantly lower N:P values. The resulting formulation was a derivative yet physicochemically distinct version of NLC_{v1}, subsequently referred to as NLC_{v2}; physicochemical properties are summarized in Table 1. Prior to the inception of NLC_{v2}, we manufactured highly concentrated versions of NLC_{v1} to increase RNA loading capacity—some containing as high as 30% w/v squalene and 1.8% w/v Dynasan 114 but with an identical S:O ratio. The latter approach allowed us to keep nanoparticle size and chemical composition constant while increasing RNA loading capacity by virtue of increased nanoparticle concentration. While this approach overcame the practical limitation of loading high amounts of RNA, it did not circumvent the use of excess formulation. As a result, in subsequent versions we reduced the amount of

squalene and Dynasan 114 to as low as 3.75% w/v squalene and 0.24% Dynasan 114, respectively, while keeping the total surfactant composition ([DOTAP] + [Span 60] + [Tween 80]) and ratio ([DOTAP]:[Span 60]:[Tween 80]) constant, effectively increasing the S:O ratio 9-fold (from 0.18 to 1.68) in NLC_{v2} relative to NLC_{v1}. Interestingly, when we screened these formulations complexed with SEAP rvRNA in vivo, we observed increasing SEAP expression with decreasing squalene concentration (Figure S6). Due to this relatively high S:O ratio, NLC_{v2} exhibited an average diameter of ~40 nm, a nearly 2-fold reduction in particle size compared to NLC_{v1} (Figure 5A), as measured by DLS. Similar to NLC_{v1}, NLC_{v2} protected rvRNA from RNase degradation (Figure 5B). To confirm the increased loading capacity of NLC_{v2}, we complexed escalating concentrations of rvRNA with NLC_{v1} or NLC_{v2} (1:1 by volume) and quantified unbound RNA by electrophoretic gel retardation assay (Figure 5C). While 100% of RNA was bound to NLC_{v1} at rvRNA concentrations less than 100 μg/mL (N:P > 20), NLC_{v2} exhibited 100% RNA-binding at rvRNA concentrations up to 10 mg/mL.

To evaluate the optimal N:P that would result in maximum SEAP expression in vitro, we complexed NLC_{v2} with SEAP-rvRNA at various N:P ratios and incubated 100-ng rvRNA doses with BHK cells overnight, as described above. We observed at least an ~5-fold reduction in optimal N:P for NLC_{v2} compared to NLC_{v1}, from >100 for NLC_{v1} to between 15 and 37 for NLC_{v2} (Figure 5D). Interestingly, the maximum SEAP expression level for NLC_{v2} was also enhanced ~2.5-fold compared to NLC_{v1}. Finally, relative to CNE (Figure 2E), NLC_{v2} provided nearly 10-fold increase in maximum SEAP expression at about 1/3 the N:P value.

We then assessed immunogenicity of ZIKV rvRNA complexed at a 10-fold higher concentration (400 μg/mL) 1:1 with NLC_{v2} (N:P = 37) in the guinea pig model, comparing 50-, 5-, and 0.5-μg doses, respectively, via IM or intradermal (ID) routes. $PRNT_{80}$ titers 28 days after a single immunization were compared with animals immunized with 50 μg naked rvRNA or 5 or 0.5 μg rvRNA formulated with NLC_{v1} (N:P = 50) (Figure 5E). We observed a dose-response trend, although there were no significant differences between doses, with the IM 50-, 5-, and 0.5-μg doses resulting in mean $PRNT_{80}$ titers of 1:761, 1:452, and 1:226, respectively, while ID doses resulted in mean $PRNT_{80}$ titers of 1:905, 1:380, and 1:269, respectively. No significant differences were observed between routes at each dose. Interestingly, significant differences were observed between NLC_{v1}- and NLC_{v2}-formulated groups at 5 μg rvRNA
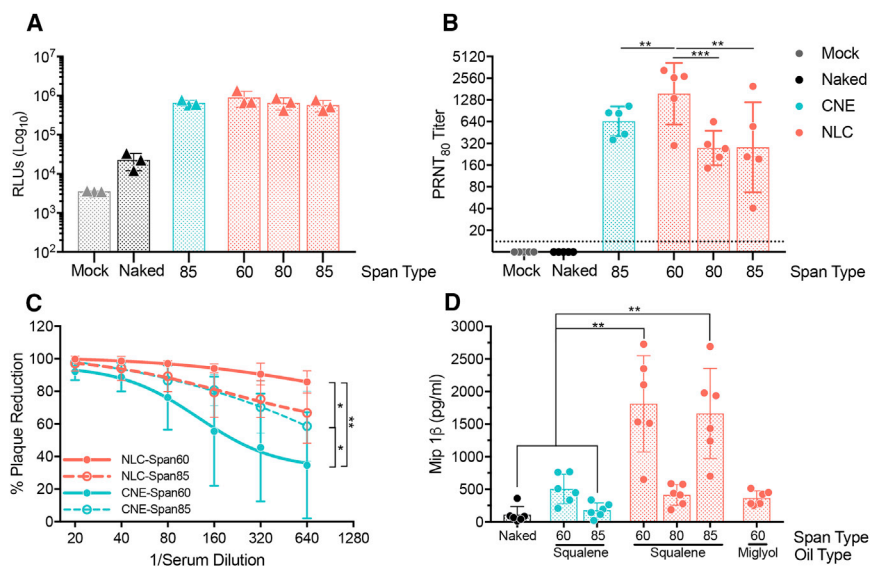
Figure 3. NLC Modifications That Modulate Immune Responses

(A) SEAP expression in peripheral serum 3 days after C57BL/6 mice (n = 3/group) were injected IM with 10% sucrose (mock) or 100 ng of SEAP rvRNA unformulated (naked) or complexed with CNE (containing Span 85) or NLCs containing Span 60, 80, or 85. Each data point is plotted as well as their mean ± SD. (B) Eighty percent reduction neutralizing antibody titers, measured by PRNT$_{80}$, 14 days after C57BL/6 mice (n = 5/group) were injected IM with 10% sucrose (mock) or 100 ng of ZIKV rvRNA unformulated (naked) or complexed with CNE (containing Span 85) or NLCs containing Span 60, 80, or 85. Each data point is plotted as well as their geometric mean ± SD. (C) ZIKV neutralization with serial dilutions of serum harvested from C57BL/6 mice (n = 5/group) 14 days after IM vaccination with 100 ng of ZIKV rvRNA complexed with NLCs or CNEs containing Span 60 or 85. Each serum dilution is plotted as mean ± SD, and a curve was fitted using a sigmoidal non-linear regression model. (D) Mip-1β concentration, as determined by ELISA, in supernatants of human peripheral blood mononuclear cells (n = 6 donors) harvested 24 hr after incubation with 40 ng ZIKV rvRNA unformulated (naked) or complexed with CNE containing Span 60 or 85 in a squalene emulsion or with NLCs containing Span 60, 80, or 85 and squalene and Dynasan or NLC containing Span 60 and miglyol and Dynasan emulsion. Two technical ELISA replicates per donor were performed, and the mean of each donor is plotted along with the mean ± SD of the six donors. Data in (A) and (B) are representative of three independent experiments. Data in (C) and (D) are representative of two independent experiments. Log$_{10}$ transform of data in (B) was analyzed by one-way ANOVA with Tukey's multiple comparison test (NLC Span 60 compared to CNE or NLC Span 85, **p < 0.008; NLC Span 60 compared to NLC Span 80, ***p = 0.0007; CNE compared to NLC Span 80 or 85, not significant). Data in (C) was analyzed by multiple two-way ANOVA with Tukey's multiple comparison test (at 1/640 serum dilution NLC Span 60 versus CNE Span 85 and CNE Span 60 versus CNE Span 85, *p < 0.05; NLC Span 60 versus CNE Span 60, **p < 0.0001). Data in (D) was analyzed by multiple one-way ANOVA with Tukey's multiple comparison test (NLC-Span 60-squalene or NLC-Span 85-squalene compared to either naked or CNE-Span 85, **p < 0.005).

dose, with NLC$_{v2}$-formulated rvRNA inducing ∼4- or ∼8-fold higher nAb titers in ID or IM routes of administration, respectively. For reference, in vitro SEAP expression at these N:P ratios was enhanced ∼8.4-fold (Figure 5D) in NLC$_{v2}$ compared to NLC$_{v1}$.

Balancing Immunogenicity with Reactogenicity

Guinea pigs have routinely been utilized to assess local adverse reactions to ID injections due to their hypersensitivity responses.[49,50] In the above guinea pig study, we observed local reactogenicity, characterized by enlarged flare-like reactions encircled by diffuse redness (wheal-like) in the 50-μg rvRNA dose formulated with NLC$_{v2}$ administered via the ID route. In order to address such reactogenicity associated with high doses of NLC$_{v2}$, we hypothesized that the ratio between formulation and RNA could be optimized to reduce reactogenicity while not impacting immunogenicity significantly. By reducing the amount of formulation, we would effectively reduce the concentration of cationic lipid, which is the likely source of reactogenicity.[47] First, we performed an in vitro experiment where various dilutions of NLC$_{v2}$ were complexed with 20 μg/mL SEAP rvRNA, resulting in a range of N:P molar ratios. These RNA and formulation complexes were then physically and biologically characterized, by measuring in vitro SEAP expression, particle size, zeta potential, and RNA binding (Figures 6A–6D). The results indicate that there are N:P ratios that result in optimal SEAP expression levels corresponding with maximal RNA binding and a constant positive zeta

potential but minimal increase in particle size. Given that, for the same formulation, there is a correlation between antigen expression and immunogenicity,[51] we hypothesized that we could expect similar nAb titers at N:P ratios (region shaded in gray in Figure 6) that corresponded to peak SEAP expression.

To characterize NLC$_{v2}$ in vivo in terms of protein expression, reactogenicity, and immunogenicity, we opted to test four to five N:P ratios, including those correlating with in vitro SEAP activity ≥5.8 log$_{10}$ relative luminescence unit (RLU) (100, 37, 15, 5.6), and an N:P of 3, outside the hypothesized optimal zone. To characterize protein expression, C57BL/6 mice were injected IM with 1,000-, 100-, and 10-ng doses of SEAP rvRNA at each N:P ratio. To characterize reactogenicity, 50 μg of rvRNA complexed with NLC$_{v2}$ at each N:P were also injected via an ID route in guinea pigs, and flare diameter was measured. Twenty-four hours after injection, mice were bled to measure serum SEAP activity, and guinea pig injection sites were measured (Figures 6E–6H). To characterize immunogenicity, ZIKV rvRNA was complexed with NLC$_{v2}$ at each N:P, and 1,000 ng or 100 ng was delivered via the IM route in mice. Mice were then bled 14 days later to quantify nAb titers (Figures 6F and 6G).

Beginning with SEAP expression in vivo, optimal N:P ratios were dependent on dose, with optimal N:P of 15 for the 1,000-ng dose, 37 for the 100-ng dose, and 100 for the 10-ng dose (Figure 6E). As
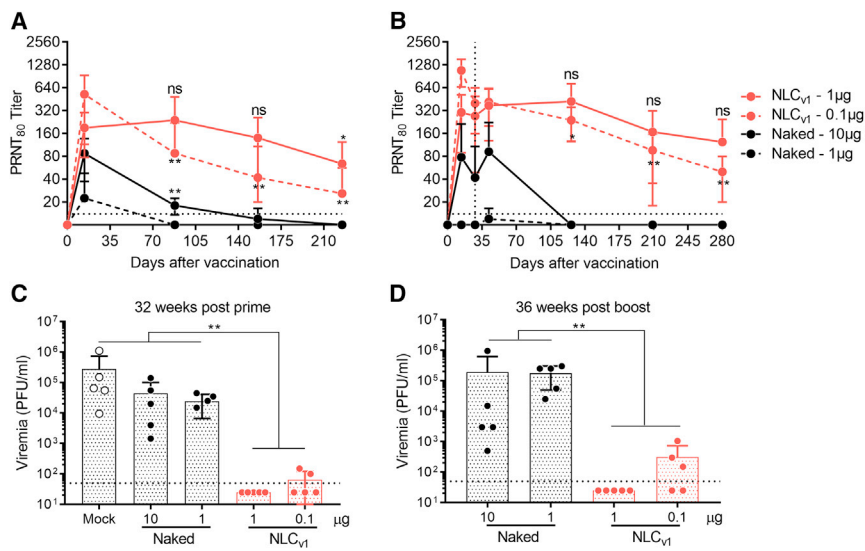
Figure 4. Durability of Neutralizing Antibody Responses following One or Two Doses of NLC-Formulated ZIKV rvRNA

C57BL/6 mice (n = 5/group) were immunized once on day 0 (A) or on day 0 and 28 (B) via the IM route with 1 or 0.1 μg ZIKV rvRNA formulated with NLC_{v1}, and neutralizing antibody titers at various time points were compared to mice immunized with 10 or 1 μg unformulated (naked) ZIKV rvRNA. Mice were then challenged 32 weeks post-prime (C) or 36 weeks post-boost (D) with 5 $\log_{10}$ PFU of ZIKV Dakar strain 41525 following antibody blockade of type I interferon as described[46] and bled 4 days later to quantify viremia by plaque assay. Data is plotted as mean ± SD of each biological replicate. Data in (A) and (C) are from the same experiment, while (B) and (D) are from a separate experiment. $\log_{10}$ transform of data in (A) and (B) was analyzed by one-way ANOVA with Tukey's multiple comparison test, comparing the mean $PRNT_{80}$ at each time point within each group to their respective peak titer at day 14 (in [A], NLC_{v1} 1 μg or naked 10 μg at days 88 and 156 compared to titers at day 14, ***p < 0.0001,

p < 0.001; in [B], NLC_{v1} 1 μg at days 126 and 209 compared to titers at day 14, *p = 0.05, ***p = 0.0001, respectively). $\log_{10}$ transform of data in (C) and (D) was analyzed by one-way ANOVA with Tukey's multiple comparison test, comparing between every group (p < 0.005).

expected, immunogenicity appeared to correlate with SEAP expression at the two doses that we compared (Figures 6F and 6G). At the 1,000-ng dose, we did not detect significant differences in nAb titers with any of the N:P ratios tested, similar to SEAP activity at those N:P ratios (Figure 6F). At the 100-ng dose, we observed no significant difference in nAb titers between N:P ratios of 37 and 15 and slight but insignificant differences in SEAP activity; however, a significant reduction in titer occurred between N:P ratios of 15 and 5.6 in a similar manner to SEAP activity (Figure 6G). In terms of reactogenicity, we observed a significant reduction in flare diameter when the N:P ratio was reduced 2.5-fold from 37 to 15 (Figure 6H). Importantly, these data suggest that reducing the N:P 2.5-fold from 37 to 15 would significantly reduce reactogenicity but minimally impact antigen expression levels and subsequent immunogenicity, especially at higher rvRNA doses. In fact, at N:P values of 15 and 37, a dose-sparing effect was observed, as there was not a significant difference in SEAP activity between 1,000- and 100-ng doses (Figure 6E). The largest differences in SEAP activity between doses was observed at low N:P ratios (Figure 6E).

Immunogenicity and Efficacy of N:P Optimized NLC_{v2} and rvRNA in C57BL/6 Mice

To assess immunogenicity and efficacy of our optimized vaccine platform, NLC_{v2} was complexed with rvRNA at a minimally reactive but immunogenic N:P ratio and used to immunize C57BL/6 mice via the IM route with 100, 30, 10, and 3 ng complexed with NLC_{v2} at an N:P of 15 (n = 14/group), and we compared responses to mice immunized with 100 ng of NLC_{v1} (n = 14)- or CNE (n = 4)-formulated rvRNA at the same N:P, which is suboptimal for their compositions. A separate study comparing NLC_{v1} and CNE at their optimal N:Ps is summarized in Figure S7. Unformulated doses of 100 and 10 ng were administered along with mock vaccination as controls (n = 14/group). Two

weeks after a single administration, mice were bled to quantify nAb titers by $PRNT_{80}$, and four mice per group were euthanized and splenocytes were isolated, stimulated with a pool of peptides corresponding to murine $CD8^+$ T cell epitopes in ZIKV prM and E,[34,52] and T cell responses measured by flow cytometry (Figures 7A, 7B, and S8).

We observed 100% seroconversion only in NLC_{v2}-formulated groups receiving 100-, 30-, and 10-ng doses with mean $PRNT_{80}$ titers of 1:604, 1:302, and 1:113, respectively. We observed 21% seroconversion in the 3-ng dose group, similar to the 100-ng NLC_{v1} group formulated at a suboptimal N:P ratio. The CNE-formulated group performed significantly better than NLC_{v1} at an N:P of 15, correlating with enhanced *in vitro* SEAP expression at lower N:P ratios (Figure 2E); however, the same dose formulated with NLC_{v2} at the same N:P resulted in ~13-fold increase in nAb titers (mean $PRNT_{80}$ of 1:604 versus 1:48, p < 0.0001).

In terms of $CD8^+$ T cell responses, we observed significant percentages of $B220_{lo}CD8^+IFN\gamma^+$ T cells, compared to mock vaccination, in mice receiving a single dose of 100 and 30 ng formulated with NLC_{v2}. These responses were significantly reduced compared to two doses of 1 μg formulated with NLC_{v1} at an N:P of 50 (Figure S7E), confirming that a prime-boost format can enhance cellular immune responses, as previously demonstrated.[53]

Finally, the remaining 10 mice per group were challenged 30 days after a single administration, as described above, and bled 4 days later to quantify viremia by plaque assay (Figure 7C). Mice were monitored daily for signs of disease and weight loss (Figures 7D and 7E). Any mice that lost more than 20% of their pre-challenge weight or appeared moribund were euthanized at the indicated
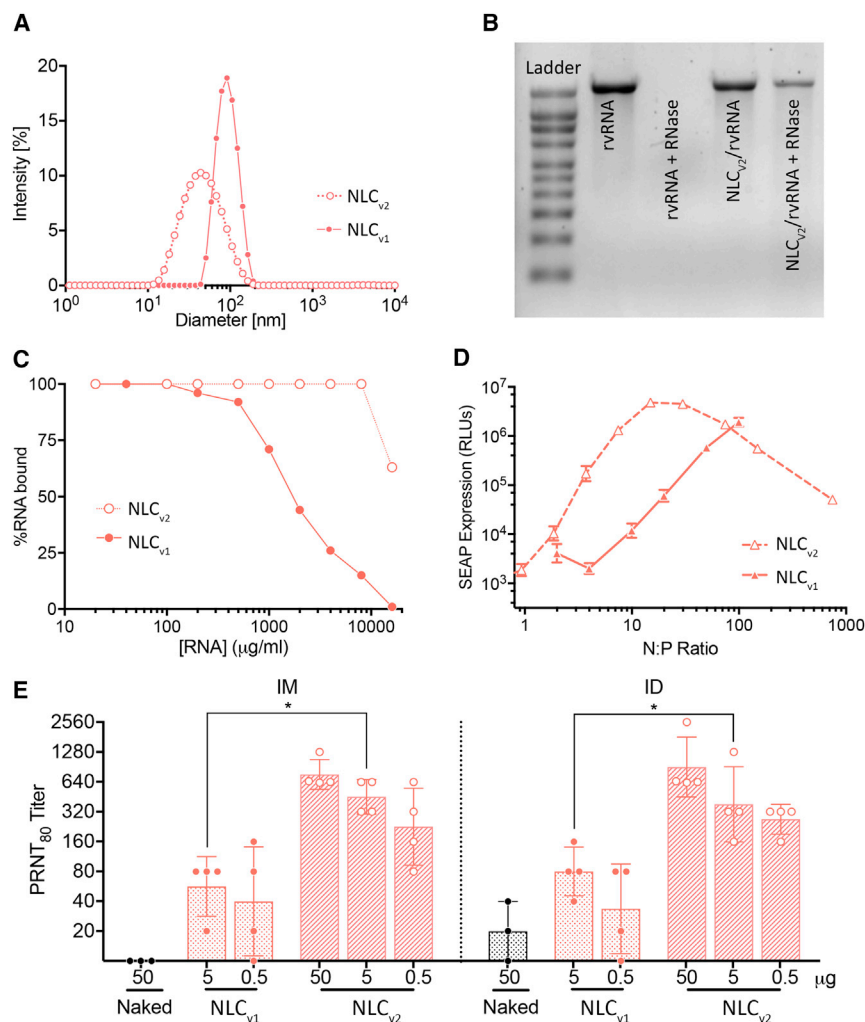
Figure 5. Characteristics of NLC_{v2} with Enhanced RNA Loading Capacity

(A) Particle size as measured by dynamic light scattering. Data are reported as Z-average. (B) Denaturing RNA agarose gel electrophoresis of untreated rvRNA (lane 2) and NLC_{v2} rvRNA (lane 4) or RNase-treated rvRNA (lane 3) and NLC_{v2} rvRNA (lane 5). Data is representative of three independent trials. (C) Percent of RNA bound to NLC_{v1} or NLC_{v2} as measured by densitometry analysis following denaturing agarose gel electrophoresis of NLC_{v1} or NLC_{v2} complexed with increasing concentrations of rvRNA. Data is representative of three independent experiments. (D) SEAP expression in BHK cell supernatant 24 hr after incubation with NLC_{v1} or NLC_{v2} complexed at various N:P ratios with SEAP rvRNA. Data is represented as mean ± SD of three biological replicates and is representative of results from three independent experiments. NLC_{v1} data reproduced from Figure 2E for comparison purposes. (E) Guinea pigs (n = 4/group) were immunized with a single 50-μg dose of unformulated ZIKV rvRNA, 5 or 0.5 μg of NLC_{v1}-formulated ZIKV rvRNA, or with 50, 5, or 0.5 μg of NLC_{v2}-formulated ZIKV rvRNA via the IM or ID routes, and serum-neutralizing antibody titers, as measured by $PRNT_{80}$, were assayed 28 days later. Each data point is reported as well as mean ± SD. Experiment performed once. Log_{10} transform of data in (E) were analyzed by one-way ANOVA with Tukey's multiple comparison test (5-μg doses between NLC_{v1} and NLC_{v2} formulations via IM, *p = 0.05, or ID, *p = 0.04).

time points (Figure 7D). All mock and unformulated 100-ng vaccinated mice experienced high levels of viremia (between 2.6 and 5.8 $\log_{10}$ PFU/mL) while 1 out of 10 mice in the 10-ng unformulated group was protected from detectable viremia (limit of detection = 50 PFU/mL). In the NLC_{v2} groups, the 100-, 30-, and 10-ng doses were 100% protected from detectable viremia, and the 3-ng dose protected six out of 10 mice; the four with detectable viremia had $PRNT_{80}$ titers <20 (Figure S9). One animal out of 10 in the 100-ng NLC_{v1}-formulated at the suboptimal N:P group was not protected from viremia. All NLC_{v1} and NLC_{v2} groups were protected from significant weight loss and death, including the 3-ng dose formulated with NLC_{v2}. Unformulated groups experienced significant weight loss, with only 10% and 20% surviving challenge up to 30 days post-challenge in the 100- and 10-ng dose groups, respectively, compared to 100% death in the mock vaccination group after 10 days post-challenge. To assess anamnestic nAb responses postchallenge, terminal serum harvested 30 days after challenge from surviving mice was assayed by PRNT. All surviving mice exhibited $PRNT_{80}$ titers >640.

DISCUSSION

Optimizing Delivery of NLC-Formulated rvRNA

Despite the widespread use of LNPs in several clinical trials,[54–56] large-scale production of LNP-formulated RNA vaccines in an emerging infectious disease scenario poses several challenges. Since LNPs encapsulate RNA, each RNA construct for a specific disease target must be formulated with its delivery vehicle at the time of manufacture, and these formulated products have limited stability, often requiring immediate use for maximum efficacy.[5] On the other hand, a two-vial approach that separates RNA and delivery vehicle until just before administration is more amenable to rapid development and availability of new vaccines, as the delivery vehicle can be stockpiled, assuming colloidal stability. Brito et al.[19] presented a two-vial approach using a CNE—an adaptation of the adjuvant MF59—to formulate RNA via simple admixing prior to administration. Here, we adopted the two-vial vaccine approach and leveraged our own knowledge in adjuvants and nanoparticles to develop an NLC formulation for delivery of rvRNA. NLC nanoparticles are comprised of a hybrid liquid squalene and solid glyceryl trimyristate (Dynasan 114) core (Figure 2A), which results in excellent colloidal stability (Figure 2C). The non-ionic hydrophobic and hydrophilic surfactants help maintain a stable nanoparticle droplet, while the cationic lipid provides the positive charge for electrostatic binding
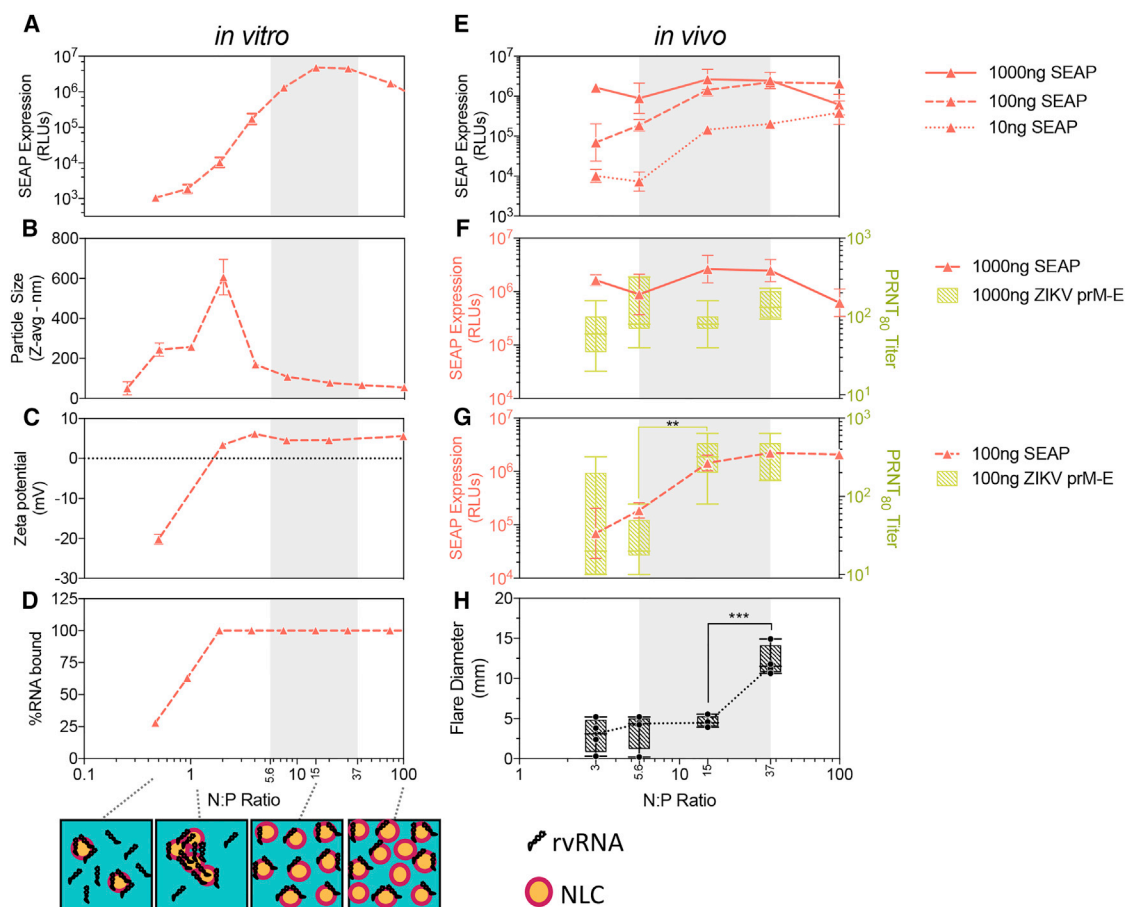
Figure 6. Mapping the Physical Relationship between NLC$_{v2}$ and rvRNA with Biological Responses, Including Gene Expression, Immunogenicity, and Reactogenicity

For *in vitro* experiments (A–D), NLC$_{v2}$ was complexed with SEAP rvRNA at various N:P ratios, and gene expression (A) was measured by SEAP assay as described above, particle size (B) and zeta potential (C) were measured by dynamic light scattering, and percent RNA binding (D) was measured by densitometry following gel electrophoresis. Data in (A)–(D) are presented as mean ± SD and are representative of at least three independent experiments. For *in vivo* experiments involving C57BL/6 mice (E–G), NLC$_{v2}$ was complexed with ZIKV or SEAP rvRNA at N:Ps of 3, 5.6, 15, and 37, and mice (n = 3/group for SEAP or n = 5/group for ZIKV) were injected via IM route with 1,000, 100, or 10 ng of SEAP rvRNA or 1,000 or 100 ng of ZIKV rvRNA. SEAP expression was determined by SEAP assay 3 days after injection (E–G), while ZIKV-neutralizing antibody titers were determined by PRNT$_{80}$ 14 days after injection (F and G). To determine reactogenicity (H), guinea pigs (n = 4/group) were injected via ID route with 50 μg ZIKV rvRNA complexed with NLC$_{v2}$ at N:Ps of 3, 5.6, 15, and 37, and flare diameter was measured 24 hr later. SEAP data in (E)–(G) are presented as mean ± SD and are from a single experiment, while PRNT$_{80}$ data in (F) and (G) are presented as mean ± SD and min and max box-whisker plots and are representative of three independent experiments. Data in (H) was from a single experiment and is presented as individual biological replicates with mean ± SD and min and max box-whisker plots. Log$_{10}$ transform of PRNT$_{80}$ data in (G) was analyzed by one-way ANOVA with Tukey's multiple comparison test (titers between N:P of 37 and 15, not significant; titers between N:P of 15 and 5.6, **p = 0.0033). Data in (H) were analyzed by one-way ANOVA with Tukey's multiple comparison test (flare diameter between N:P of 37 and 15, ***p = 0.0004; between N:P of 15 and 5.6 or 3, not significant). A cartoon depicting a hypothesized model of the physical interaction between NLC and rvRNA supported by the data is presented in (D).

of RNA. Since RNA binds to the NLC surface, we sought to elucidate the role of surface chemistry. We made sequential modifications to surface components and studied the corresponding effect on RNA delivery, protein expression, and immunogenicity, ultimately leading to the selection of a specific NLC composition that provided maximum protection against ZIKV. First, we evaluated the role of the non-ionic polyethylene glycol (PEG)ylated surfactant Tween 80 on RNA protection and SEAP expression; our results showed that NLCs with relatively high Tween 80 content or ~70% of total surfactant and cationic lipid mass did not offer protection from RNase chal-

lenge, but formulations with approximately half that (35%) did (Figure S3). This finding was not surprising, as PEG chains in Tween 80 can inhibit non-specific or electrostatic binding with macromolecules,[57] which is likely the cause for the lack of RNase protection observed with a relatively high amount of Tween 80. As expected, SEAP expression for rvRNA delivered with a high percent Tween 80 formulation, which did not offer RNase protection, was no different to unformulated rvRNA (Figure S3). Our findings suggest that while Tween 80 was necessary to formulate stable NLCs, a high amount relative to other surfactants was detrimental to RNA
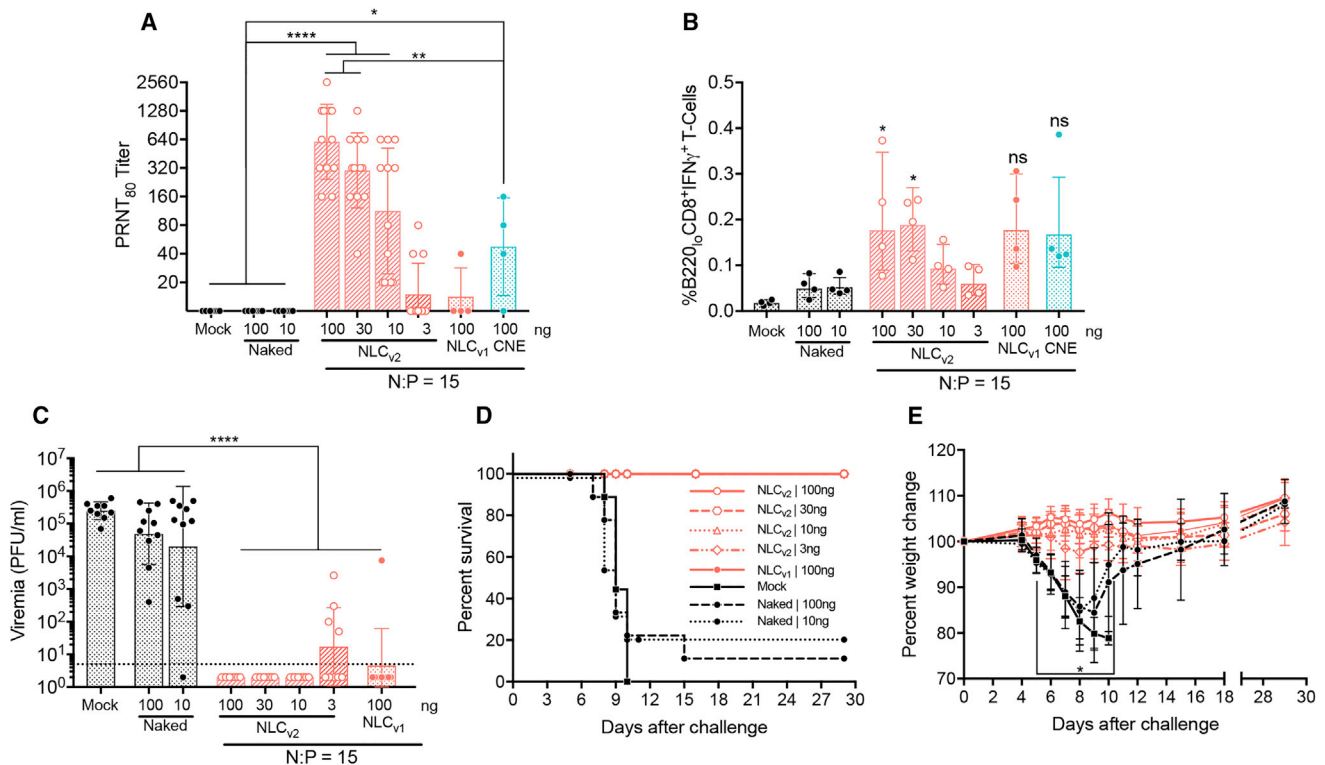
Figure 7. Immunogenicity and Efficacy of Optimized rvRNA and NLC$_{v2}$ Complexes in C57BL/6 Mice

NLC$_{v2}$ was complexed with rvRNA encoding ZIKV prM and E at an N:P of 15, and 100-, 30-, 10-, and 3-ng doses were administered to C57BL/6 mice via a single IM injection (n = 14/group) and 14 days later bled to assess neutralizing antibody titers by PRNT$_{80}$ (A) or euthanized (n = 4/group) to quantify percent antigen-specific B220$_{lo}$CD8$^+$IFNγ^+ T cells in total splenocytes (B) compared to mock-vaccinated mice, 100 or 10 ng naked rvRNA (n = 14/group), or 100 ng formulated with NLC$_{v1}$ (n = 14) or CNE (n = 4) at an N:P of 15. Data are presented as individual values as well as mean ± SD. Thirty days after immunization, the remaining 10 mice per group were challenged with 5 log$_{10}$ PFU of ZIKV Dakar strain 41525 following antibody blockade of type I interferon as described[46] and bled 4 days later to quantify viremia by plaque assay (C). Data are presented as individual values as well as mean ± SD. Mice were monitored daily for survival (D) and weight loss (E). Data in (E) are presented as mean ± SD. Log$_{10}$ transform of data in (A) and (C) was analyzed by one-way ANOVA with Tukey's multiple comparison test (PRNT$_{80}$ titers in [A] between control groups—mock and unformulated 100- and 10-ng doses and NLC$_{v2}$ formulated 100-, 30-, and 10-ng doses, ****p < 0.0001, or CNE formulated 100 ng, *p = 0.04; between NLC$_{v2}$-formulated 100- and 30-ng doses and CNE-formulated 100 ng, **p = 0.006; viremia titers in [C] between control groups—mock, unformulated 100- and 10-ng doses, and all NLC$_{v2}$- or NLC$_{v1}$-formulated doses, ****p < 0.0001). Data in (E) was analyzed by two-way ANOVA with Tukey's multiple comparison test (on days 5–10 the percent weight change between control groups—mock or 100- and 10-ng naked rvRNA, and all formulated groups, *p < 0.05). Data in (A)–(C) are representative of two independent experiments.

binding and protection. As a result, for subsequent studies, we elected to use NLC formulations with Tween 80 no greater than 35% of the total surfactant and cationic lipid mass fraction.

Optimizing Immunogenicity of NLC-Formulated rvRNA

Nucleic-acid-based vaccines have enabled a shift from a dependence on vaccination with exogenously produced protein antigens to utilizing the vaccinee's host-cell machinery to endogenously produce vaccine antigens, upon which an immune response can be mounted. Inherent in this approach, immunogenicity tends to be dependent on effective delivery and a threshold level of antigen expression. However, with regard to the latter, the magnitude of immune responses can be enhanced through mechanisms that are either dependent or independent of increasing antigen expression. For example, Leitner et al.[58] demonstrated equivalent reporter gene expression levels between traditional plasmid DNA expression and DNA-launched

rvRNA expression but immunogenicity was enhanced in the latter approach. This enhancement was attributed to innate immune stimulation by double-stranded replicative RNA intermediates and was independent of the amount of antigen expressed. On the other hand, Pepini et al.[51] recently demonstrated that rvRNA-mediated antigen expression levels correlated with changes in immunogenicity. When IFNAR deficient ($IFNAR^{-/-}$) mice were administered rvRNA expressing SEAP, expression levels were enhanced $\sim$100-fold compared to wild-type (WT) mice administered the same rvRNA, and this correlated with a significant, albeit small, increase in antigen-specific antibody titers. In either of these studies, the effect of the nucleic acid delivery vehicle was not addressed.

To date, a number of studies have elucidated the effects of lipid-based RNA delivery vehicles on innate immune activation with an emphasis on type I interferon (IFN) induction and subsequent antiviral[59] and

adjuvant-like[60] effects. Given the deleterious effects of type I IFN on rvRNA replication and antigen expression,[51] delivery vehicles that are immunologically inert or those that may adjuvant immune responses via alternative mechanisms independent of activation of antiviral responses are more desirable. For example, CNE, which is similar in composition to MF59, a commercial adjuvant with a well-characterized mechanism of action and a wealth of clinical data,[43] induced high levels of innate immune cell infiltrate to the site of immunization and it was proposed that this response was likely important for the observed immunogenicity.[19] However, these studies could not rule out the effect of efficient rvRNA delivery and antigen expression as the primary mechanism of immunogenicity, as they observed similar levels of protein expression and immunogenicity between viral and CNE delivery, but low levels of innate immune cell infiltrate was observed with viral delivery.[19]

In our evaluation of various hydrophobic sorbitan ester surfactants, or Spans, used for stabilizing NLCs, we identified compositions that appear to adjuvant immune responses independently of RNA delivery. NLCs containing 0.5% w/v of Span 60 (sorbitan monostearate), Span 80 (sorbitan monooleate), or Span 85 (sorbitan trioleate) offered similar protection from RNase challenge and comparable rvRNA delivery, as determined by similar in vivo SEAP expression levels (Figure 3A). However, the adaptive immune response was significantly modulated, with nAb titers in both CNE and NLC groups utilizing Span 80 or Span 85 significantly lower compared to NLC$_{v1}$ utilizing Span 60 (Figure 3B). We subsequently demonstrated that Span 60 in the context of NLCs induced human PBMCs to secrete elevated levels of Mip-1β, while Span 60 in the context of CNE or non-squalene (Miglyol 810)-based NLCs did not, suggesting the specific combination of Span 60, Dyanasan 114, and squalene were important for this adjuvant effect. Mip-1β has been implicated in the adjuvant mechanism of action of MF59 and has subsequently been used as surrogate marker of adjuvant potency in release assays during adjuvant manufacture.[42–44,61] More work is needed to characterize the downstream effects of chemokines such as Mip-1β on cellular infiltrate to sites of rvRNA and NLC administration. These findings are significant because in addition to encoding antigens for prophylactic vaccination, RNA platforms have applications in delivery of self-antigens, such as antibodies, where minimizing immune responses to RNA-encoded antibodies could enhance the half-life of expressed antibodies.[62] To that end, we are actively trying to elucidate the mechanism by which hydrophobic surfactants in NLC formulations modulate immune responses in vivo, and more work is needed to screen additional components for similar effects.

NLC-Formulated Zika Vaccine
In the context of a Zika vaccine, where maximizing immunogenicity to rvRNA-encoded antigens is the primary objective, we utilized the Span 60 variants of NLC (NLC$_{v1}$ and NLC$_{v2}$) to characterize immune responses and assess efficacy in mice. Given the deleterious role of type I IFN in rvRNA-mediated antigen expression and subsequent effect on measured immune responses, including antibody titers,[51] we decided to quantify immune responses in immunocompetent

C57BL/6 mice instead of the more commonly used interferon-deficient mouse models (e.g., A129, AG129) that are susceptible to ZIKV infection.[31,36,45] In order to assess efficacy in WT mice, we transiently blocked IFN alpha receptors by passive mAb transfer prior to and after challenge with ZIKV.[46] In contrast to previous RNA-based Zika vaccine studies that utilized C57BL/6 mice to assess immunogenicity, we demonstrated 100% seroconversion following a single IM administration with as low as 10 ng and 100% protection from death with as low as 3 ng. In terms of protection against viremia, a single dose as low as 10 ng was able to at least reduce the duration of viremia as ZIKV was not detected 4 days after challenge; however, viremia at earlier time points were not assessed due to the constraints of the animal model.[46] Non-replicating mRNA-based vaccines formulated in LNPs have required either a single 30-μg dose administered through four sites of injection[35] or a prime and boost with 10 μg to achieve 100% seroconversion in this same animal model.[37] Furthermore, we demonstrated that a single 1- or 0.1-μg dose formulated with NLC$_{v1}$ resulted in durable immune responses, with nAb persisting to at least 5 months after vaccination (Figure 4A). Interestingly, while the lower 0.1-μg dose resulted in higher peak nAb titers, the durability of these immune responses and their ability to protect against viremia 9–10 months after immunization was diminished compared to the 1-μg dose. More work is needed to characterize the long-term immunogenicity and efficacy of our second-generation NLC$_{v2}$.

While an obvious benefit to dose sparing includes a reduced cost per dose, a less obvious reason, but relevant to the field of RNA delivery, is the requirement for less formulation and thus reduced reactogenicity. In our optimized NLC$_{v2}$ formulation, utilizing an optimal N:P molar ratio of 15 translates to 30 ng of DOTAP for every 1 ng of rvRNA. For reference, we only began to see significant reactogenicity at 100,000-fold higher doses of DOTAP (3,720 μg). By increasing the potency per copy of delivered RNA through a self-amplifying strategy, we are able to indirectly reduce the reactogenicity by relying on less formulation for effective intracellular delivery. More work is needed to understand how the physical properties of NLCs relate to optimal N:P ratios and elucidate those properties that correlate with lowering the optimal N:P. In our work characterizing NLC$_{v1}$ and NLC$_{v2}$, we observed a reduction of optimal N:P from >50 to 15 (Figure 5D). Concomitant with that reduction was increasing the S:O molar ratio from 0.18 to 1.68, which reduced the particle size from ~100 nm to ~40 nm (Table 1). Since the total oil content between NLC$_{v1}$ and NLC$_{v2}$ differs only slightly (~20%), in theory, reducing the particle size by approximately 2.5-fold amounts to approximately 12-fold increase in the number of nanoparticles, assuming spherical geometry. It is likely that the smaller size and theoretically higher number of nanoparticles in NLC$_{v2}$ enables distribution of surface-bound rvRNA copies to a greater number of cells. We are actively pursuing additional studies to verify our hypothesis and elucidate other physicochemical variables that correlate strongly with further reduction in optimal N:P.

This study demonstrated a two-vial approach with single-dose efficacy for Zika. All studies to date that utilized the admix formulation, CNE, demonstrated efficacy, albeit for other disease indications,

following two or more doses.[10,19,63,64] However, it should be noted that these prior studies complexed CNE with rvRNA at an N:P of either 7[19,63] or 10;[10,64] in our hands, these N:P ratios resulted in sub-optimal antigen expression (Figure 2E). These findings highlight the importance of characterizing antigen expression as a function of N:P and that identifying formulations with optimal antigen expression at the lowest N:P ratios could potentially reduce reactogenicity while maintaining sufficient immunogenicity.

MATERIALS AND METHODS
Cells and Viruses
293T, BHK-21, and Vero cells (American Type Culture Collection, Rockville, MD) were maintained at 37°C with 5% CO_2 in DMEM containing 10% (v/v) heat-inactivated fetal bovine serum (FBS), sodium pyruvate (1 mM), penicillin (100 U/mL), and streptomycin (100 μg/mL). All cell lines were pre-screened for mycoplasma contamination.

Plasmid Constructs
A plasmid encoding an SP6 promoter followed by the 5′ and 3′ UTRs and nonstructural genes of Venezuelan equine encephalitis virus (VEEV) strain TC-83 as well as enhanced GFP under the control of the VEEV subgenomic promoter was kindly provided by Dr. Scott Weaver (UTMB). We then replaced the SP6 promoter with a T7 promoter using standard cloning techniques, termed pT7-VEE-Rep-GFP. A fragment encoding codon-optimized prM and E genes from ZIKV strain H/PF/2013 was synthesized and cloned into pUC57 (Genscript). Using a Q5 mutagenesis kit (New England Biolabs), we then inserted a kozak sequence followed by either the JEV or ZIKV signal sequence (ss) using the following primers: JEVss-FWD (5′-gctggcctccctggctgtggtcattgcctgcgctggagcaGCCGAG GTGACCAGGAGAGG-3′) and JEVss-REV (5′-cacatgattgatccggcact cctcttgcccatggcggcggcGTGAGCTGGCGGCGGGTG-3′), or ZIKVss-FWD (5′-ggaatcgtgggcctgctgctgaccacagcaatggcaGCCGAGGTGAC CAGGAGAGG-3′) and ZIKVss-REV (5′-cacggatgtgtctgctcctctccgca tggcggcggcGTGAGCTGGCGGCGGGTG-3′). This combined frag-ment encoding either the JEVss or ZIKVss followed by ZIKV prM and E genes was then PCR amplified with the primers ZIKV-prM-E-FWD (5′-AATGGACTACgacatagtcgccgccgccatg-3′) and ZIKV-prM-E-REV (5′-GCGGTTTTTGACAccgcggTCAGGCAGACACG GCG-3′) and cloned between PflFI and SacII sites in pT7-VEE-Rep-GFP, using infusion enzyme mix (Clontech), resulting in pT7-VEE-Rep-JEVss-ZIKV-prM-E or pT7-VEE-Rep-ZIKVss-ZIKV-prM-E plasmids. pT7-VEE-Rep-SEAP was constructed by PCR amplification and cloned between PflFI and SacII sites in pT7-VEE-Rep-GFP as described above. All plasmids were confirmed by Sanger sequencing.

RNA Production
Following transformation and amplification in Top10 cells (Invitro-gen) and isolation using maxi-prep kits (QIAGEN), plasmids were linearized by restriction digest with NotI enzyme (New England Biolabs) and purified using phenol-chloroform. RNA was then tran-scribed *in vitro* using T7 megascript kit (Invitrogen) followed by

lithium chloride precipitation and capping with a vaccinia capping kit (New England Biolabs). Capped transcripts were then precipitated in lithium chloride and resuspended in nuclease-free water to a final concentration of 1 μg/μL and analyzed by agarose-gel electrophoresis. All RNA was aliquoted and stored at −80°C.

Formulation Production
Both CNE and NLC nanoparticle formulations consist of an oil core that is stabilized in an aqueous buffer using suitable surfactants. The oil phase was composed of squalene—the liquid phase of the oil core—a non-ionic sorbitan ester surfactant, either sorbitan trioleate (Span 85) or sorbitan monostearate (Span 60), the cationic lipid DOTAP (N-[1-(2,3-Dioleoyloxy)propyl]-N,N,N-trimethylammo-nium chloride) and in the case of NLC formulations, the solid lipid glyceryl trimyristate (Dynasan 114). The aqueous phase was a 10-mM sodium citrate trihydrate buffer containing the non-ionic PEGylated surfactant Tween 80. Separately, the two phases were heated and equilibrated to 60°C in a bath sonicator. Following com-plete dissolution of the solid components, the oil and aqueous phases were mixed at 5,000 rpm in a high-speed laboratory emulsifier (Silver-son Machines) to produce a crude mixture containing micron-sized oil droplets. Further particle size reduction was achieved by high-shear homogenization in a M-110P microfluidizer (Microfluidics). The colloid mixtures were processed at 30,000 psi for five discrete microfluidization passes. The final pH was between 6.5 and 6.8. Formulations were terminally filtered with a 0.2-μm polyethersulfone membrane syringe filter and stored at 2°C–8°C. Chemical composi-tion and physical properties of exemplary formulations are provided in Table 1.

Physical Characterization of rvRNA + NLC Complexes
Hydrodynamic diameter of nanoparticle formulations was deter-mined using the DLS technique (Zetasizer Nano ZS, Malvern Instru-ments). Formulations were diluted 1:100 with water in triplicate prep-arations and measured in a disposable polystyrene cuvette (standard operating procedure [SOP] parameters, material RI = 1.59, dispersant RI (water) = 1.33, T = 25°C, viscosity (water) = 0.887 centipoise [cP], measurement angle = 173° backscatter, measurement position = 4.65 mm, automatic attenuation). For zeta potential measurement, formulations were diluted 1:100 in triplicates and loaded in a dispos-able DTS1070 (Malvern Instruments)-folded capillary cell. The following SOP parameters were used: material RI = 1.59, dispersant RI (water) = 1.33, viscosity (water) = 0.887 cP, T = 25°C, automatic attenuation and voltage selection. The intensity-weighted Z-average diameter, polydispersity index (PDI), and zeta potential values for each formulation, averaged from three measurements/replicate (nine total measurements), are reported in Table 1. Particle size of formulated RNA (NLC + RNA or CNE + RNA complex) at different N:P values was measured in triplicate using the Zetasizer Auto Plate Sampler (APS, Malvern Instruments) in a 384-well plate configura-tion. Zeta potential of formulated RNA at different N:P values was measured in triplicate following the same method described above for formulation alone. NLC binding capacity was determined using a gel retardation assay. In brief, NLC and rvRNA complexes were

prepared at various N:P values and electrophoresed as is in 1% agarose gel. Standard concentrations were used to quantify unbound or excess rvRNA migrating in the gel.

RNase Challenge Assay

ZIKV-rvRNA was complexed with NLC_{v1} and NLC_{v2} at N:P ratios of 50 and 15, respectively, and placed on ice for 30 min. After diluting the NLC_{v2} complex using nuclease-free water, complexes containing 1 μg of rvRNA at 20 μg/mL were treated with 50 ng of RNase A (Thermo Scientific) for 30 min at room temperature, followed by an incubation with 5 μg of recombinant Proteinase K (Thermo Scientific) for 10 min at 55°C. RNA was then extracted using an equal volume of 25:24:1 phenol:chloroform:isoamyl alcohol (Invitrogen). After vortexing, samples were centrifuged at $17,000 \times g$ for 15 min. The supernatant were collected and mixed 1:1 with Glyoxal load dye (Invitrogen) and heated at 50°C for 15 min. The equivalent of 200 ng of RNA were loaded and run on a denatured 150 mL 1% agarose gel in Northern Max Gly running buffer (Invitrogen) at 120 V for 45 min. Gels were imaged using a ChemiDoc MP imaging system (BioRad). The intensity of the intact rvRNA band was compared to phenol:chloroform:isoamyl extracted RNA from complexes that were not subjected to RNase and Proteinase K treatment. Additional controls included rvRNA alone with and without RNase and Proteinase K treatment at a 200-ng rvRNA load.

Complexing Conditions for *In Vitro* and *In Vivo* Experiments

In N:P optimization experiments, NLC_{v1} or NLC_{v2} was serially diluted in 10 mM citrate buffer and complexed 1:1 with rvRNA diluted to 20 μg/mL in a nuclease-free 10% sucrose solution (to maintain isotonicity without using an ionic agent such as saline). rvRNA was added to formulation and gently pipetted up and down to ensure complete mixing. The complex was incubated for 30 min on ice, resulting in a range of N:P molar ratios. These complexes were then further diluted in 10% sucrose to achieve the desired doses. For *in vitro* stimulation of human PBMCs, complexed formulations were diluted 1:125. For vaccination studies utilizing NLC_{v1} or CNE at an N:P of 50, rvRNA was diluted to 40 μg/mL in 10% sucrose and complexed 1:1 with formulation. For the guinea pig study where NLC_{v2} was utilized at an N:P of 37, rvRNA was diluted to 400 μg/mL in 10% sucrose and complexed 1:1 with formulation. For vaccine studies that utilized NLC_{v2} at an N:P of 15, rvRNA was diluted to 1,000 μg/mL in 10% sucrose and complexed 1:1 with formulation. Complexes were then utilized neat or diluted in 10% sucrose for the desired doses as indicated in the figure legends.

ZIKV VLP Characterization

ZIKV-rvRNA was complexed with NLC_{v1} at an N:P of 50, and 100 ng was incubated on a monolayer of 293T cells in a 6-well plate in Optimem media for 4 hr, followed by replacement with complete media and a final 20-hr incubation. Supernatants were then harvested and overlaid onto a 20% sucrose solution and pelleted by ultracentrifugation at $100,000 \times g$ for 2 hr at 10°C (OPTIMA MAX-XP, Beckman). Pellets were then resuspended in PBS and analyzed by SDS-PAGE and western blot. To detect ZIKV proteins following transfer to nitro-

cellulose membrane, anti-ZIKV mouse immune ascitic fluids (WRCEVA, UTMB) were utilized at a 1:5,000 dilution and a 1:4,000 dilution of the secondary reagent, goat anti-mouse immunoglobulin G (IgG)-horseradish peroxidase (HRP) (Southern Biotech), was utilized to visualize protein bands. For transmission electron microscopy (TEM) evaluation, the above 293T supernatants were pelleted through a 20% sucrose solution onto a 70% sucrose cushion by ultracentrifugation at $100,000 \times g$ for 2 hr at 10°C. The interphase was then harvested and sucrose replaced with PBS by filtration through a 100-kDa Amicon filter (Millipore). A drop of undiluted filtrate was dried on a 300-mesh holey carbon grid, stained with uranyl acetate, and examined in a 200-kV FEI TEM for the presence of ZIKV VLPs.

SEAP Assay

To characterize protein expression from formulated rvRNA, we utilized a SEAP reporter system. Twenty-four hours after BHK cells were incubated with formulated SEAP rvRNA, supernatants were harvested, and SEAP activity was measured by NovaBright Phospha-Light assay, per manufacturer's instructions (Thermo Fisher).

nAb Titers

$PRNT_{80}$ were performed on Vero cells as previously described[65] using ZIKV strain FSS 13025 as the control virus. In brief, a stock of ZIKV FSS 13025 was diluted to $\sim 1 \times 10^3$ PFU/mL, and the titer was confirmed by plaque assay on Vero cells. Samples were heat inactivated at 56°C for 30 min then serially diluted in DMEM containing 1% FBS. All diluted samples were then diluted an additional 2-fold by the addition of ~ 200 PFU of ZIKV, mixed, and incubated at 37°C for 1 hr, then transferred to 90% confluent monolayers of Vero cells in 6-well plates (Costar) and incubated at 37°C for 1 hr. Overlay containing 1% agarose in DMEM with 1% non-essential amino acids, 1% L-glutamine, and 1% gentamycin was then pipetted into each well, and plates were incubated for 3 days at 37°C. Cells were then fixed in 10% formaldehyde, and plaques visualized following crystal violet staining.

Human PBMC Assay

Studies involving human donors were approved by the western institutional review board. Heparinized whole blood was attained from six normal donors upon informed consent and PBMCs were isolated as previously described.[44] One million cells per 150 μL volume of serum-free RPMI were plated into U-bottom tissue culture (TC)-grade 96-well plates and formulation and rvRNA complexes were added to the cells in a 50 μL volume and incubated at 37°C. Twenty-four hours later, plates were centrifuged for 10 min at 1.8 k rpm, and supernatants were harvested and stored at −20°C. Mip-1β ELISA was performed as previously described.[44]

Animal Studies

All animal studies were approved by the Infectious Disease Research Institute Institutional Animal Care and Use Committee. The facility where animal studies were conducted is accredited by the Association for Assessment and Accreditation of Laboratory Animal Care,

International and follows guidelines set forth by the Guide for the Care and Use of Laboratory Animals, National Research Council, 2011. All sample sizes were determined based on power analysis assuming LD100 challenge doses and subsequent survival rates of 0.99 versus 0.01 with $\alpha = 0.05$ using a one-sided Fisher's exact test. Mice were non-specifically and blindly distributed into their respective groups.

To quantify protein expression or immunogenicity in an immunocompetent mouse model, 4-week-old female C57BL/6 mice (Charles River) were vaccinated IM with a 1:1 mixture containing formulation and rvRNA encoding SEAP or ZIKV prM and E in the rear quadriceps muscle in a total volume of 50 μL. At various time points, indicated in the figure legends, blood was collected via the retro-orbital route, and serum was harvested following low-speed centrifugation and stored at $-20°C$ until $PRNT_{80}$ titers or serum-SEAP activity was determined as described above.

To assess immunogenicity and tolerability in guinea pigs, 400−450 g Hartley guinea pigs (Charles River) were vaccinated IM or ID utilizing Nanopass Micronjet600 needles (Nanopass Technologies) with a 1:1 mixture containing NLC and rvRNA encoding ZIKV prM and E in the rear quadriceps muscle in a total volume of 250 μL. Twenty-four hours later, the diameter of the ID injection-site flare was measured. Blood was collected at the time points indicated in the figure legends via the femoral vein and serum was harvested following low-speed centrifugation and stored at $-20°C$ until $PRNT_{80}$ titers were determined as described above.

Statistics
Statistical analysis was performed using GraphPad Prism software (version 7.0c) and RStudio (version 0.99.491). Data distribution and variance were evaluated for normality and similiarity with or without transformation by qqplot and boxplot analyses. One-way and two-way ANOVAs with Tukey's multiple comparison test were used as described in the figure legends.

SUPPLEMENTAL INFORMATION
Supplemental Information includes nine figures and can be found with this article online at https://doi.org/10.1016/j.ymthe.2018.07.010.

AUTHOR CONTRIBUTIONS
Conceptualization, J.H.E., A.P.K., D.T.S., N.V.H.; Methodology, J.H.E., A.P.K., J.G., B.G., J.A., M.A., C.B.F., N.V.H.; Investigation, J.H.E., A.P.K., J.G., B.G., J.A., M.A., E.G., J.F.-S., E.L.; Writing – Original Draft, J.H.E., A.P.K.; Writing – Review & Editing, J.H.E., A.P.K., D.T.S., C.B.F., S.G.R., R.N.C., N.V.H.; Funding Acquisition, R.N.C., D.T.S., S.G.R., N.V.H.; Supervision, R.K., R.N.C., C.B.F., D.T.S., S.G.R., N.V.H.

ACKNOWLEDGMENTS

REFERENCES
1. Wolff, J.A., Malone, R.W., Williams, P., Chong, W., Acsadi, G., Jani, A., and Felgner, P.L. (1990). Direct gene transfer into mouse muscle in vivo. Science 247, 1465–1468.

2. Kaczmarek, J.C., Kowalski, P.S., and Anderson, D.G. (2017). Advances in the delivery of RNA therapeutics: from concept to clinical reality. Genome Med. 9, 60.

3. DeFrancesco, L. (2017). The 'anti-hype' vaccine. Nat. Biotechnol. 35, 193–197.

4. Hekele, A., Bertholet, S., Archer, J., Gibson, D.G., Palladino, G., Brito, L.A., Otten, G.R., Brazzoli, M., Buccato, S., Bonci, A., et al. (2013). Rapidly produced SAM(®) vaccine against H7N9 influenza is immunogenic in mice. Emerg. Microbes Infect. 2, e52.

5. Ball, R.L., Bajaj, P., and Whitehead, K.A. (2016). Achieving long-term stability of lipid nanoparticles: examining the effect of pH, temperature, and lyophilization. Int. J. Nanomedicine 12, 305–315.

6. Charlton Hume, H.K., and Lua, L.H.L. (2017). Platform technologies for modern vaccine manufacturing. Vaccine 35 (35 Pt A), 4480–4485.

7. Plotkin, S., Robinson, J.M., Cunningham, G., Iqbal, R., and Larsen, S. (2017). The complexity and cost of vaccine manufacturing - An overview. Vaccine 35, 4064–4071.

8. Myhr, A.I. (2017). DNA Vaccines: Regulatory Considerations and Safety Aspects. Curr. Issues Mol. Biol. 22, 79–88.

9. Lechardeur, D., and Lukacs, G.L. (2006). Nucleocytoplasmic transport of plasmid DNA: a perilous journey from the cytoplasm to the nucleus. Hum. Gene Ther. 17, 882–889.

10. Bogers, W.M., Oostermeijer, H., Mooij, P., Koopman, G., Verschoor, E.J., Davis, D., Ulmer, J.B., Brito, L.A., Cu, Y., Banerjee, K., et al. (2015). Potent immune responses in rhesus macaques induced by nonviral delivery of a self-amplifying RNA vaccine expressing HIV type 1 envelope with a cationic nanoemulsion. J. Infect. Dis. 211, 947–955.

11. Geall, A.J., Verma, A., Otten, G.R., Shaw, C.A., Hekele, A., Banerjee, K., Cu, Y., Beard, C.W., Brito, L.A., Krucker, T., et al. (2012). Nonviral delivery of self-amplifying RNA vaccines. Proc. Natl. Acad. Sci. USA 109, 14604–14609.

12. Petsch, B., Schnee, M., Vogel, A.B., Lange, E., Hoffmann, B., Voss, D., Schlake, T., Thess, A., Kallen, K.J., Stitz, L., and Kramps, T. (2012). Protective efficacy of in vitro synthesized, specific mRNA vaccines against influenza A virus infection. Nat. Biotechnol. 30, 1210–1216.

13. Li, J., He, Y., Wang, W., Wu, C., Hong, C., and Hammond, P.T. (2017). Polyamine-Mediated Stoichiometric Assembly of Ribonucleoproteins for Enhanced mRNA Delivery. Angew. Chem. Int. Ed. Engl. 56, 13709–13712.

14. Lehto, T., Ezzat, K., Wood, M.J.A., and El Andaloussi, S. (2016). Peptides for nucleic acid delivery. Adv. Drug Deliv. Rev. 106 (Pt A), 172–182.

15. Schott, J.W., Morgan, M., Galla, M., and Schambach, A. (2016). Viral and Synthetic RNA Vector Technologies and Applications. Mol. Ther. 24, 1513–1527.

16. Barefoot, B., Thornburg, N.J., Barouch, D.H., Yu, J.S., Sample, C., Johnston, R.E., Liao, H.X., Kepler, T.B., Haynes, B.F., and Ramsburg, E. (2008). Comparison of multiple vaccine vectors in a single heterologous prime-boost trial. Vaccine 26, 6108–6118.

17. Liao, F., Xu, H., Torrey, N., Road, P., and Jolla, L. (2015). Lipid Nanoparticles for Gene Delivery. Adv. Genet. 2, 1–21.

18. Kau, K.J., Dorkin, J.R., Yang, J.H., Heartlein, M.W., DeRosa, F., Mir, F.F., Fenton, O.S., and Anderson, D.G. (2015). Optimization of Lipid Nanoparticle Formulations for mRNA Delivery in Vivo with Fractional Factorial and Definitive Screening Designs. Nano Lett 15, 7300–7306.

19. Brito, L.A., Chan, M., Shaw, C.A., Hekele, A., Carsillo, T., Schaefer, M., Archer, J., Seubert, A., Otten, G.R., Beard, C.W., et al. (2014). A cationic nanoemulsion for the delivery of next-generation RNA vaccines. Mol. Ther. 22, 2118–2129.

20. Dwarki, V.J., Malone, R.W., and Verma, I.M. (1993). Cationic liposome-mediated RNA transfection. Methods Enzymol. 217, 644–654.

21. Foy, B.D., Kobylinski, K.C., Chilson Foy, J.L., Blitvich, B.J., Travassos da Rosa, A., Haddow, A.D., Lanciotti, R.S., and Tesh, R.B. (2011). Probable non-vector-borne transmission of Zika virus, Colorado, USA. Emerg. Infect. Dis. 17, 880–882.

22. Pinto-Díaz, C.A., Rodríguez, Y., Monsalve, D.M., Acosta-Ampudia, Y., Molano-González, N., Anaya, J.M., and Ramírez-Santana, C. (2017). Autoimmunity in Guillain-Barré syndrome associated with Zika virus infection and beyond. Autoimmun. Rev. 16, 327–334.

23. Anaya, J.-M., Rodríguez, Y., Monsalve, D.M., Vega, D., Ojeda, E., González-Bravo, D., Rodríguez-Jiménez, M., Pinto-Díaz, C.A., Chaparro, P., Gunturiz, M.L., et al. (2017). A comprehensive analysis and immunobiology of autoimmune neurological syndromes during the Zika virus outbreak in Cúcuta, Colombia. J. Autoimmun. 77, 123–138.

24. Cugola, F.R., Fernandes, I.R., Russo, F.B., Freitas, B.C., Dias, J.L., Guimarães, K.P., Benazzato, C., Almeida, N., Pignatari, G.C., Romero, S., et al. (2016). The Brazilian Zika virus strain causes birth defects in experimental models. Nature 534, 267–271.

25. Rasmussen, S.A., Jamieson, D.J., Honein, M.A., and Petersen, L.R. (2016). Zika virus and birth defects—reviewing the evidence for causality. N. Engl. J. Med. 374, 1981–1987.

26. Pradhan, D., Yadav, M., Verma, R., Khan, N.S., Jena, L., and Jain, A.K. (2017). Discovery of T-cell Driven Subunit Vaccines from Zika Virus Genome: An Immunoinformatics Approach. Interdiscip. Sci. 9, 468–477.

27. To, A., Medina, L.O., Mfuh, K.O., Lieberman, M.M., Wong, T.A.S., Namekar, M., Nakano, E., Lai, C.Y., Kumar, M., Nerurkar, V.R., and Lehrer, A.T. (2018). Recombinant Zika Virus Subunits Are Immunogenic and Efficacious in Mice. MSphere 3, e00576–e17.

28. Modjarrad, K., Lin, L., George, S.L., Stephenson, K.E., Eckels, K.H., De La Barrera, R.A., Jarman, R.G., Sondergaard, E., Tennant, J., Ansel, J.L., et al. (2018). Preliminary aggregate safety and immunogenicity results from three trials of a purified inactivated Zika virus vaccine candidate: phase 1, randomised, double-blind, placebo-controlled clinical trials. Lancet 391, 563–571.

29. Abbink, P., Larocca, R.A., De La Barrera, R.A., Bricault, C.A., Moseley, E.T., Boyd, M., Krilova, M., Li, Z., Ng'ang'a, D., Nanayakkara, O., et al. (2016). Protective efficacy of multiple vaccine platforms against Zika virus challenge in rhesus monkeys. Science 353, 1129–1132.

30. Xie, X., Yang, Y., Muruato, A.E., Zou, J., Shan, C., Nunes, B.T., Medeiros, D.B., Vasconcelos, P.F., Weaver, S.C., Rossi, S.L., and Shi, P.Y. (2017). Understanding zika virus stability and developing a chimeric vaccine through functional analysis. MBio 8, 1–14.

31. Shan, C., Muruato, A.E., Nunes, B.T.D., Luo, H., Xie, X., Medeiros, D.B.A., Wakamiya, M., Tesh, R.B., Barrett, A.D., Wang, T., et al. (2017). A live-attenuated Zika virus vaccine candidate induces sterilizing immunity in mouse models. Nat. Med. 23, 763–767.

32. Dowd, K.A., Ko, S.Y., Morabito, K.M., Yang, E.S., Pelc, R.S., DeMaso, C.R., Castilho, L.R., Abbink, P., Boyd, M., Nityanandam, R., et al. (2016). Rapid development of a DNA vaccine for Zika virus. Science 354, 237–240.

33. Larocca, R.A., Abbink, P., Peron, J.P., Zanotto, P.M., Iampietro, M.J., Badamchi-Zadeh, A., Boyd, M., Ng'ang'a, D., Kirilova, M., Nityanandam, R., et al. (2016). Vaccine protection against Zika virus from Brazil. Nature 536, 474–478.

34. Muthumani, K., Griffin, B.D., Agarwal, S., Kudchodkar, S.B., Reuschel, E.L., Choi, H., Kraynyak, K.A., Duperret, E.K., Keaton, A.A., Chung, C., et al. (2016). In vivo protection against ZIKV infection and pathogenesis through passive antibody transfer and active immunisation with a prMEnv DNA vaccine. NPJ Vaccines 1, 16021.

35. Pardi, N., Hogan, M.J., Pelc, R.S., Muramatsu, H., Andersen, H., DeMaso, C.R., Dowd, K.A., Sutherland, L.L., Scearce, R.M., Parks, R., et al. (2017). Zika virus protection by a single low-dose nucleoside-modified mRNA vaccination. Nature 543, 248–251.

36. Richner, J.M., Jagger, B.W., Shan, C., Fontes, C.R., Dowd, K.A., Cao, B., Himansu, S., Caine, E.A., Nunes, B.T.D., Medeiros, D.B.A., et al. (2017). Vaccine Mediated Protection Against Zika Virus-Induced Congenital Disease. Cell 170, 273–283.e12.

37. Richner, J.M., Himansu, S., Dowd, K.A., Butler, S.L., Salazar, V., Fox, J.M., Julander, J.G., Tang, W.W., Shresta, S., Pierson, T.C., et al. (2017). Modified mRNA vaccines protect against Zika virus infection. Cell 168, 1114–1125.e10.

38. Müller, R.H., Alexiev, U., Sinambela, P., and Keck, C.M. (2016). Nanostructured lipid carriers (NLC): the second generation of solid lipid nanoparticles. In Percutaneous Penetration Enhancers Chemical Methods in Penetration Enhancement: Nanocarriers, N. Dragicevic and H.I. Maibach, eds. (Springer), pp. 161–185.

39. Ljungberg, K., and Liljeström, P. (2015). Self-replicating alphavirus RNA vaccines. Expert Rev. Vaccines 14, 177–194.

40. Baronti, C., Piorkowski, G., Charrel, R.N., Boubis, L., Leparc-Goffart, I., and de Lamballerie, X. (2014). Complete coding sequence of zika virus from a French polynesia outbreak in 2013. Genome Announc. 2, e00500–e00514.

41. Chang, G.J.J., Hunt, A.R., Holmes, D.A., Springfield, T., Chiueh, T.S., Roehrig, J.T., and Gubler, D.J. (2003). Enhancing biosynthesis and secretion of premembrane and envelope proteins by the chimeric plasmid of dengue virus type 2 and Japanese encephalitis virus. Virology 306, 170–180.

42. Calabro, S., Tritto, E., Pezzotti, A., Taccone, M., Muzzi, A., Bertholet, S., De Gregorio, E., O'Hagan, D.T., Baudner, B., and Seubert, A. (2013). The adjuvant effect of MF59 is due to the oil-in-water emulsion formulation, none of the individual components induce a comparable adjuvant effect. Vaccine 31, 3363–3369.

43. Calabro, S., Tortoli, M., Baudner, B.C., Pacitto, A., Cortese, M., O'Hagan, D.T., De Gregorio, E., Seubert, A., and Wack, A. (2011). Vaccine adjuvants alum and MF59 induce rapid recruitment of neutrophils and monocytes that participate in antigen transport to draining lymph nodes. Vaccine 29, 1812–1823.

44. Seubert, A., Monaci, E., Pizza, M., O'Hagan, D.T., and Wack, A. (2008). The adjuvants aluminum hydroxide and MF59 induce monocyte and granulocyte chemoattractants and enhance monocyte differentiation toward dendritic cells. J. Immunol. 180, 5402–5412.

45. Rossi, S.L., Tesh, R.B., Azar, S.R., Muruato, A.E., Hanley, K.A., Auguste, A.J., Langsjoen, R.M., Paessler, S., Vasilakis, N., and Weaver, S.C. (2016). Characterization of a Novel Murine Model to Study Zika Virus. Am. J. Trop. Med. Hyg. 94, 1362–1369.

46. Smith, D.R., Hollidge, B., Daye, S., Zeng, X., Blancett, C., Kuszpit, K., Bocan, T., Koehler, J.W., Coyne, S., Minogue, T., et al. (2017). Neuropathogenesis of Zika Virus in a Highly Susceptible Immunocompetent Mouse Model after Antibody Blockade of Type I Interferon. PLoS Negl. Trop. Dis. 11, e0005296.

47. Lv, H., Zhang, S., Wang, B., Cui, S., and Yan, J. (2006). Toxicity of cationic lipids and cationic polymers in gene delivery. J. Control. Release 114, 100–109.

48. Desbien, A.L., Reed, S.J., Bailor, H.R., Dubois Cauwelaert, N., Laurance, J.D., Orr, M.T., Fox, C.B., Carter, D., Reed, S.G., and Duthie, M.S. (2015). Squalene emulsion potentiates the adjuvant activity of the TLR4 agonist, GLA, via inflammatory caspases, IL-18, and IFN-γ. Eur. J. Immunol. 45, 407–417.

49. Wilhelmsen, C.L., and Waag, D.M. (2000). Guinea pig abscess/hypersensitivity model for study of adverse vaccination reactions induced by use of Q fever vaccines. Comp. Med. 50, 374–378.

50. Maurer, T. (2007). Guinea pigs in hypersensitivity testing. Methods 41, 48–53.

51. Pepini, T., Pulichino, A.M., Carsillo, T., Carlson, A.L., Sari-Sarraf, F., Ramsauer, K., Debasitis, J.C., Maruggi, G., Otten, G.R., Geall, A.J., et al. (2017). Induction of an IFN-Mediated Antiviral Response by a Self-Amplifying RNA Vaccine: Implications for Vaccine Design. J. Immunol. 198, 4012–4024.

52. Elong Ngono, A., Vizcarra, E.A., Tang, W.W., Sheets, N., Joo, Y., Kim, K., Gorman, M.J., Diamond, M.S., and Shresta, S. (2017). Mapping and Role of the CD8+ T Cell Response During Primary Zika Virus Infection in Mice. Cell Host Microbe 21, 35–46.

53. Knudsen, M.L., Ljungberg, K., Kakoulidou, M., Kostic, L., Hallengärd, D., García-Arriaza, J., Merits, A., Esteban, M., and Liljeström, P. (2014). Kinetic and phenotypic analysis of CD8+ T cell responses after priming with alphavirus replicons and homologous or heterologous booster immunizations. J. Virol. 88, 12438–12451.

54. Kanasty, R., Dorkin, J.R., Vegas, A., and Anderson, D. (2013). Delivery materials for siRNA therapeutics. Nat. Mater. 12, 967–977.

55. Kanasty, R.L., Whitehead, K.A., Vegas, A.J., and Anderson, D.G. (2012). Action and reaction: the biological response to siRNA and its delivery vehicles. Mol. Ther. *20*, 513–524.

56. Rietwyk, S., and Peer, D. (2017). Next-Generation Lipids in RNA Interference Therapeutics. ACS Nano *11*, 7572–7586.

57. Kim, T.W., Kim, Y.J., Chung, H., Kwon, I.C., Sung, H.C., and Jeong, S.Y. (2002). The role of non-ionic surfactants on cationic lipid mediated gene transfer. J. Control. Release *82*, 455–465.

58. Leitner, W.W., Hwang, L.N., deVeer, M.J., Zhou, A., Silverman, R.H., Williams, B.R., Dubensky, T.W., Ying, H., and Restifo, N.P. (2003). Alphavirus-based DNA vaccine breaks immunological tolerance by activating innate antiviral pathways. Nat. Med. *9*, 33–39.

59. Nguyen, D.N., Chen, S.C., Lu, J., Goldberg, M., Kim, P., Sprague, A., Novobrantseva, T., Sherman, J., Shulga-Morskaya, S., de Fougerolles, A., et al. (2009). Drug delivery-mediated control of RNA immunostimulation. Mol. Ther. *17*, 1555–1562.

60. Nguyen, D.N., Mahon, K.P., Chikh, G., Kim, P., Chung, H., Vicari, A.P., Love, K.T., Goldberg, M., Chen, S., Krieg, A.M., et al. (2012). Lipid-derived nanoparticles for immunostimulatory RNA adjuvant delivery. Proc. Natl. Acad. Sci. USA *109*, E797–E803.

61. Misquith, A., Fung, H.W., Dowling, Q.M., Guderian, J.A., Vedvick, T.S., and Fox, C.B. (2014). In vitro evaluation of TLR4 agonist activity: formulation effects. Colloids Surf. B Biointerfaces *113*, 312–319.

62. Pardi, N., Secreto, A.J., Shan, X., Debonera, F., Glover, J., Yi, Y., Muramatsu, H., Ni, H., Mui, B.L., Tam, Y.K., et al. (2017). Administration of nucleoside-modified mRNA encoding broadly neutralizing antibody protects humanized mice from HIV-1 challenge. Nat. Commun. *8*, 14630.

63. Brazzoli, M., Magini, D., Bonci, A., Buccato, S., Giovani, C., Kratzer, R., Zurli, V., Mangiavacchi, S., Casini, D., Brito, L.M., et al. (2015). Induction of Broad-Based Immunity and Protective Efficacy by Self-amplifying mRNA Vaccines Encoding Influenza Virus Hemagglutinin. J. Virol. *90*, 332–344.

64. Maruggi, G., Chiarot, E., Giovani, C., Buccato, S., Bonacci, S., Frigimelica, E., Margarit, I., Geall, A., Bensi, G., and Maione, D. (2017). Immunogenicity and protective efficacy induced by self-amplifying mRNA vaccines encoding bacterial antigens. Vaccine *35*, 361–368.

65. Beaty, B.J.J., Calisher, C.H.H., and Shope, R.E.E. (1989). Arboviruses. In Diagnostic Procedures for Viral, Rickettsial and Chlamydial Infections, N.J.J. Schmidt and R.W.W. Emmons, eds. (American Public Health Association), pp. 797–855.